Theoretical Aspects of Microchannel Acoustofluidics

Thermoviscous Corrections to the Radiation Force and Streaming

Tribler, Peter Muller; Bruus, Henrik

Published in:
I U T A M. Procedia

Link to article, DOI:
10.1016/j.piutam.2014.01.035

Publication date:
2014

Document Version
Publisher's PDF, also known as Version of record

Available online at www.sciencedirect.com

ScienceDirect

Procedia IUTAM 10 (2014) 410 – 415

Procedia IUTAM

www.elsevier.com/locate/procedia

23rd International Congress of Theoretical and Applied Mechanics

Theoretical aspects of microchannel acoustofluidics: Thermoviscous corrections to the radiation force and streaming

Peter Barkholt Muller, Henrik Bruus*

Department of Physics, Technical University of Denmark, DTU Physics Buildig 309, Kongens Lyngby DK-2800, Denmark

Abstract

We study the effects of the temperature dependence of viscosity and density on the acoustic radiation force and the boundary-driven acoustic streaming in microchannel acoustofluidics. The acoustic streaming slip velocity for the bulk flow is calculated numerically taking these thermoviscous effects into account inside the micrometer-thin acoustic boundary layer and compare the results to recent analytical work in the literature. The acoustic radiation force is calculated for the case of an ultrasound wave scattering on a compressible, spherical particle suspended in a viscous, thermal conducting fluid. Using Prandtl–Schlichting boundary-layer theory, we include the viscosity and the volume thermal expansion coefficient of the fluid and derive an analytical expression for the radiation force. The resulting force (valid for particle radius and boundary layers much smaller than the acoustic wavelength) is analyzed for microchannel acoustophoresis.

Selection and/or peer-review under responsibility of the Organizing Committee of The 23rd International Congress of Theoretical and Applied Mechanics, ICTAM2012

Keywords: microparticle acoustophoresis, acoustic streaming, acoustic radiation force, thermoviscous acoustofluidics

1. Background and governing equations

With recent developments in microfabrication technologies allowing for integration of ultrasound resonators in lab-on-a-chip systems, the acoustic radiation force has received renewed attention as a label- and contact-free way to manipulate particles [1, 2]. Traditionally, acoustic streaming is treated in the isothermal case, and the acoustic radiation force has been modeled using the inviscid theory of the acoustic radiation force. This approach is approximately correct for liquids having a small volume thermal expansion coefficient and for particles of radius a much larger than the thicknesses δ and δ_{th} of the viscous and thermal boundary layers, in which dissipation plays a dominant role. However, given the recent experimental advances including improved accuracy [3] and the use of smaller particles [4] as well as recent analytical results for both streaming [5] and radiation [6], it is relevant to re-visit the theoretical analysis taking thermoviscous effects into account.

*Corresponding author. *E-mail address:* henrik.bruus@nanotech.dtu.dk.

Selection and/or peer-review under responsibility of the Organizing Committee of The 23rd International Congress of Theoretical and Applied Mechanics, ICTAM2012
doi:10.1016/j.piutam.2014.01.035

1.1. First-order equations

Briefly, and to establish our notation [7], the full acoustic problem in a fluid, which before the presence of any acoustic wave is quiescent with constant temperature T_0, density ρ_0, and pressure p_0, is described by the four scalar fields pressure p, temperature T, density ρ and entropy per mass unit s as well as the velocity vector field $\boldsymbol{v}$. The two thermodynamic relations

$$\mathrm{d}\rho = \frac{\gamma}{c_0^2}\,\mathrm{d}p - \alpha\rho\,\mathrm{d}T, \quad \text{and} \quad \mathrm{d}s = \frac{C_p}{T}\,\mathrm{d}T - \frac{\alpha}{\rho}\,\mathrm{d}p, \quad \text{with} \quad \alpha = -\frac{1}{\rho_0}\left(\frac{\partial\rho}{\partial T}\right)_p, \tag{1}$$

can be used to eliminate ρ and s, so that we only need to deal with the acoustic perturbations in temperature T, pressure p, and velocity $\boldsymbol{v}$. Here c_0 is the (isentropic) sound speed, C_p the specific heat at constant pressure, and γ (≈ 1.01 for water at 293 K) is the ratio of specific heats . To first order (subscript "1") in the acoustic perturbation, the independent fields are

$$T = T_0 + T_1, \qquad p = p_0 + p_1, \qquad \text{and} \qquad \boldsymbol{v} = \boldsymbol{v}_1, \tag{2}$$

while the dependent fields, density ρ and viscosity η, are

$$\rho = \rho_0 + \rho_1 = \rho_0 + \frac{\gamma}{c_0^2}\,p_1 - \alpha\rho_0\,T_1 \qquad \text{and} \qquad \eta = \eta_0 + \eta_1 = \eta_0 + (\partial_p\eta)_0\,p_1 + (\partial_T\eta)_0\,T_1. \tag{3}$$

The thermodynamic heat transfer equation for T_1, the kinematic continuity equation expressed in terms of p_1, and the dynamic Navier–Stokes equation for the velocity field $\boldsymbol{v}_1$, become

$$\partial_t T_1 = D_{\mathrm{th}}\nabla^2 T_1 + \frac{\alpha T_0}{\rho_0 C_p}\,\partial_t p_1, \tag{4a}$$

$$\partial_t p_1 = \frac{\rho_0 c_0^2}{\gamma}, \left[\alpha\partial_t T_1 - \boldsymbol{\nabla}\cdot\boldsymbol{v}_1\right], \tag{4b}$$

$$\rho_0\partial_t\boldsymbol{v}_1 = -\boldsymbol{\nabla}p_1 + \eta_0\nabla^2\boldsymbol{v}_1 + \beta\eta_0\,\boldsymbol{\nabla}(\boldsymbol{\nabla}\cdot\boldsymbol{v}_1). \tag{4c}$$

Here (with values for water at room temperature given in parenthesis), D_{th} is the thermal diffusivity (1.44×10^{-7} m^2/s), α is the volume thermal expansion coefficient (2.97×10^{-4} K^{-1}), C_p is the heat capacity (4.18×10^3 J $\cdot$ kg$^{-1}\cdot$ K^{-1}), ρ_0 is the density (998 kg/m^3), η_0 is the dynamic viscosity (0.89×10^{-3} Pa $\cdot$ s), and β is the viscosity ratio ($\approx 1/3$). A further simplification can be obtained when assuming all first-order fields to have harmonic time dependence $\mathrm{e}^{-\mathrm{i}\omega t}$, because then p_1 can be eliminated inserting Eq. (4b) with $\partial_t p_1 = -\mathrm{i}\omega p_1$ into Eq. (4a) and (4c). After using the thermodynamic identity $T_0\alpha^2c_0^2/C_p = \gamma - 1$ and introducing the kinematic viscosity $\nu = \eta_0/\rho_0$, we arrive at

$$\mathrm{i}\omega T_1 + \gamma D_{\mathrm{th}}\nabla^2 T_1 = \frac{1-\gamma}{\alpha}\,\boldsymbol{\nabla}\cdot\boldsymbol{v}_1 \qquad \text{and} \qquad \mathrm{i}\omega\boldsymbol{v}_1 + \nu\nabla^2\boldsymbol{v}_1 + \nu\left(\beta + \mathrm{i}\frac{c_0^2}{\gamma\nu\omega}\right)\boldsymbol{\nabla}(\boldsymbol{\nabla}\cdot\boldsymbol{v}_1) = \frac{c_0^2\alpha}{\gamma}\,\boldsymbol{\nabla}T_1. \tag{5}$$

From Eq. (5) arise the thermal and the viscous penetration depth δ_{th} and δ, respectively (values for 2 MHz in water),

$$\delta_{\mathrm{th}} = \sqrt{\frac{2D_{\mathrm{th}}}{\omega}} \approx 0.15\ \mu\mathrm{m} \qquad \text{and} \qquad \delta = \sqrt{\frac{2\nu}{\omega}} \approx 0.38\ \mu\mathrm{m}. \tag{6}$$

1.2. Second-order equations for acoustic streaming

The continuity and Navier–Stokes equations to second-order (subscript "2") in the acoustic perturbation become

$$\partial_t\rho_2 = -\rho_0\boldsymbol{\nabla}\cdot\boldsymbol{v}_2 - \boldsymbol{\nabla}\cdot(\rho_1\boldsymbol{v}_1), \tag{7a}$$

$$\begin{aligned}\rho_0\partial_t\boldsymbol{v}_2 = &-\boldsymbol{\nabla}p_2 + \eta_0\nabla^2\boldsymbol{v}_2 + \beta\eta_0\boldsymbol{\nabla}(\boldsymbol{\nabla}\cdot\boldsymbol{v}_2)\\ &+ \boldsymbol{\nabla}\cdot\Big\{\eta_1\big[\boldsymbol{\nabla}\boldsymbol{v}_1 + (\boldsymbol{\nabla}\boldsymbol{v}_1)^{\mathrm{T}} + (\beta-1)(\boldsymbol{\nabla}\cdot\boldsymbol{v}_1)\boldsymbol{I}\big]\Big\} - \rho_1\partial_t\boldsymbol{v}_1 - \rho_0(\boldsymbol{v}_1\cdot\boldsymbol{\nabla})\boldsymbol{v}_1,\end{aligned} \tag{7b}$$

where $\boldsymbol{I}$ and superscript "T" represents the unit tensor and transposing, respectively. We note that there is no coupling to the second-order thermal field T_2, and consequently thermal effects enter only through the temperature-dependent first-order fields ρ_1, η_1 and $\boldsymbol{v}_1$.

In a typical experiment on microparticle acoustophoresis, the microsecond timescale of the ultrasound oscillations is not resolved. It therefore suffices to treat only the time-averaged equations over one oscillation period (angled brackets $\langle \dots \rangle$ below) [8]. The time average of the second-order continuity equation and Navier–Stokes equation is

$$\rho_0 \boldsymbol{\nabla} \cdot \langle \boldsymbol{v}_2 \rangle = - \boldsymbol{\nabla} \cdot \langle \rho_1 \boldsymbol{v}_1 \rangle, \tag{8a}$$

$$\begin{aligned} -\boldsymbol{\nabla}\langle p_2\rangle + \eta_0 \nabla^2 \langle \boldsymbol{v}_2\rangle + \beta\eta_0 \boldsymbol{\nabla}(\boldsymbol{\nabla}\cdot\langle \boldsymbol{v}_2\rangle) = &-\langle \boldsymbol{\nabla}\eta_1 \cdot [\boldsymbol{\nabla}\boldsymbol{v}_1 + (\boldsymbol{\nabla}\boldsymbol{v}_1)^{\mathrm{T}}]\rangle - (\beta-1)\langle(\boldsymbol{\nabla}\cdot\boldsymbol{v}_1)\boldsymbol{\nabla}\eta_1\rangle \\ &- \langle \eta_1 \nabla^2 \boldsymbol{v}_1\rangle - \beta\langle \eta_1 \boldsymbol{\nabla}(\boldsymbol{\nabla}\cdot\boldsymbol{v}_1)\rangle + \langle \rho_1 \partial_t \boldsymbol{v}_1\rangle + \rho_0\langle(\boldsymbol{v}_1\cdot\boldsymbol{\nabla})\boldsymbol{v}_1\rangle. \end{aligned} \tag{8b}$$

It is seen that products of first-order fields act as source terms (at the right-hand sides) for the second-order fields (at the left-hand sides). We note that for complex-valued fields $A(t)$ and $B(t)$ with harmonic time-dependence $\mathrm{e}^{-\mathrm{i}\omega t}$, the time average is given by the real-part rule $\langle A(t)B(t)\rangle = \frac{1}{2}\,\mathrm{Re}\,[A(0)^*\, B(0)]$, where the asterisk represents complex conjugation. We implement and solve these equations numerically using the software Comsol Multiphysics 4.2a as described in our recently published work [7].

The second-order problem was solved analytically in the isothermal case of the infinite parallel-plate channel in the yz-plane by Rayleigh [9], Landau and Lifshitz [10]. Assuming a first-order bulk velocity field with only the horizontal y-component v_{1y} being non-zero and of the form $v_{1y} = U_1 \cos(2\pi y/\lambda)\, \mathrm{e}^{-\mathrm{i}\omega t}$, the resulting y-component $\langle v_{2y}^{\mathrm{bnd}}\rangle$ of $\langle \boldsymbol{v}_2\rangle$ just outside the boundary layers becomes

$$\langle v_{2y}^{\mathrm{bnd},0}\rangle = \frac{3}{8}\,\frac{U_1^2}{c_0}\,\sin\!\left(\frac{4\pi y}{\lambda}\right). \tag{9}$$

Recently, Rednikov and Sadhal [5] extended this analysis by including the oscillating thermal field as well as temperature dependence of the viscosity. They found that the slip velocity condition changed to

$$\langle v_{2y}^{\mathrm{bnd,T}}\rangle = \left(1 + \frac{2B_T}{3}\right)\langle v_{2y}^{\mathrm{bnd},0}\rangle, \quad \text{with} \quad B_T = (\gamma-1)\left[1 - (\partial_T \eta)_p\,\frac{1}{\eta_0 \alpha}\right]\frac{\sqrt{\nu/D_{\mathrm{th}}}}{1+\nu/D_{\mathrm{th}}}. \tag{10}$$

Thus the inclusion of the thermoviscous effects leads to a temperature-dependent pre-factor multiplying the temperature-independent result.

1.3. Second-order equations for the acoustic radiation force

A general mathematical expression for the acoustic radiation force (wavelength λ) with thermoviscous corrections is given by Doinikov [11]. However, he presented analytical results in closed form only for particles with a thick boundary layer ($a \ll \delta, \delta_{\mathrm{th}} \ll \lambda$) and with a thin boundary layer ($\delta, \delta_{\mathrm{th}} \ll a \ll \lambda$). Here, we extend his analysis and present analytical results in closed form for any particle size ($a, \delta, \delta_{\mathrm{th}} \ll \lambda$). The resulting radiation force is analyzed using parameter values typically employed in microparticle acoustophoresis in microchannels.

The time average of the first-order fields is zero, so the acoustic radiation force $\boldsymbol{F}^{\mathrm{rad}}$ is the time average of the second-order acoustic fields. The general expression for $\boldsymbol{F}^{\mathrm{rad}}$ is the following surface integral [11]

$$\boldsymbol{F}^{\mathrm{rad}} = \oint_{\mathrm{surf}} \langle \boldsymbol{\sigma}_2 - \rho_0 \boldsymbol{v}_1 \boldsymbol{v}_1\rangle \cdot \boldsymbol{n}\,\mathrm{d}a \quad \text{(integral over the equilibrium surface of the sphere)}, \tag{11}$$

where $\boldsymbol{\sigma}_2$ is the stress tensor of the fluid to second order, and $\boldsymbol{n}$ is the outward surface normal vector.

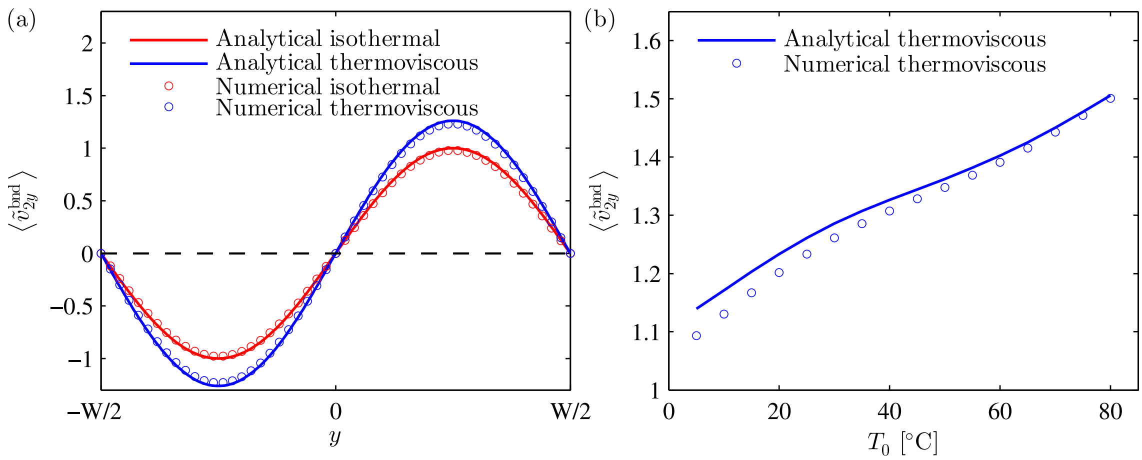

Fig. 1. (a) The amplitude of the acoustic streaming slip velocity, at $T_0 = 25$ °C, normalized according to Eq. (12). The analytical thermoviscous result by Rednikov and Sadhal [5] (blue line) is 26 % larger than the classical isothermal result by Rayleigh [9, 10] (red line). Our numerical results obtained using Comsol for the thermoviscous and isothermal models are shown with blue and red circles, respectively; (b) Amplitude of the thermoviscous acoustic streaming slip velocity as function of the equilibrium temperature T_0.

2. Results

2.1. Thermoviscous acoustic streaming slip velocity

The analytical isothermal results by Rayleigh [9], Landau and Lifshitz [10], and the analytical thermoviscous results by Rednikov and Sadhal [5] are compared with our numerics in Fig. 1. The boundary streaming velocities have been normalized to Rayleigh's result according to

$$\langle \tilde{v}_{2y}^{\mathrm{bnd}} \rangle = \frac{\langle v_{2y}^{\mathrm{bnd}} \rangle}{\langle v_{2y}^{\mathrm{bnd},0} \rangle}. \tag{12}$$

In Fig. 1a is shown the boundary slip velocity $\langle v_{2y}^{\mathrm{bnd}} \rangle$ along a segment of width $W{=}\lambda/2$ of the infinite parallel plates channel. The analytical prediction by Rednikov and Sadhal, taking into account temperature-induced first-order variations η_1 of the viscosity, is 26% larger than the isothermal prediction by Lord Rayleigh. The thermoviscous numerical results are 23% larger than Rayleigh's result, while the isothermal numerical results are 2% smaller. We have ensured that the numerical results have converged. In Fig. 1 b are shown the results of thermoviscous simulations carried out for different equilibrium temperatures T_0. All equilibrium values of the material parameters used in the numerical model are changed according to the value of T_0, and in Table 1 they are shown for $T_0 = 25$°C. For high temperatures there is an almost exact match between the numerical and analytical results, while an increasing difference is observed when going to lower temperatures. We have no apparent explanation for this discrepancy, however the general trend of the numerical and analytical results are in good agreement.

2.2. Thermoviscous acoustic radiation force

The first-order scattering problem splits into a monopole term (the vibration of a stationary, compressible sphere) and a dipole term (the translation of a moving, rigid sphere). With this decomposition, the problem reduces to find the corresponding scattering coefficients, which then are inserted into expression (11) for $\boldsymbol{F}^{\mathrm{rad}}$. Some relevant parameters are $\tilde{\rho}$ (particle/fluid density ratio), $\tilde{\kappa}$ (particle/fluid compressibility ratio), $\tilde{\delta} = \delta/a$, $\tilde{\delta}_{\mathrm{th}} = \delta_{\mathrm{th}}/a$, and $ka = 2\pi a/\lambda$.

Table 1. Acoustic parameters. Values are taken from Comsol 4.2a material library for water at $T_0 = 25\,^o$C

Parameter	Symbol	Value	Unit
Density	ρ_0	998	$\mathrm{kg{\cdot}m^{-3}}$
Speed of sound	c_0	1495	$\mathrm{m{\cdot}s^{-1}}$
Viscosity	η_0	0.893	$\mathrm{m \cdot Pa{\cdot}s}$
Thermal conductivity	k_{th}	0.603	$\mathrm{W{\cdot}m^{-1}{\cdot}K^{-1}}$
Specific heat capacity	c_p	4183	$\mathrm{J{\cdot}kg^{-1}{\cdot}K^{-1}}$
Thermal expansion coefficient	α	2.97×10^{-4}	$\mathrm{K^{-1}}$
Thermal diffusivity	D_{th}	1.44×10^{-7}	$\mathrm{m^2{\cdot}s^{-1}}$
Specific heat capacity ratio	γ	1.01	

2.2.1. Fluids without thermal expansion

For a fluid without thermal expansion ($\alpha = 0, \gamma = 1$), the thermal and acoustic fields in Eq. (5) decouple, and $T_1 = 0$. The term $\langle \boldsymbol{\sigma}_2 \rangle$ in Eq. (11) is written as products of first-order fields, and by matching the first-order solutions for p_1 and $\boldsymbol{v}_1$ in the inviscid bulk with those inside the boundary layer, we calculate $\boldsymbol{F}^{\mathrm{rad}}$ for arbitrary standing and traveling waves. For the special case of a planar standing wave, $p_{\mathrm{in}} = p_{\mathrm{a}} \cos(kz)$, we find

$$\begin{aligned} F^{\mathrm{rad}}_{\mathrm{1D}}(z) &= 4\pi\left(\frac{f_1}{3} + \frac{f_2^{\mathrm{r}}}{2}\right) a^3 k E_{\mathrm{ac}} \sin(2kz), \quad f_1 = 1 - \tilde{\kappa}, \quad f_2^{\mathrm{r}} = \mathrm{Re}\left[\frac{2(1-\varGamma)(\tilde{\rho}-1)}{2\tilde{\rho}+1-3\varGamma}\right], \\ \varGamma &= -\frac{3}{2}\left[1 + \mathrm{i}(1+\tilde{\delta})\right]\tilde{\delta}, \end{aligned} \tag{13}$$

where E_{ac} is the acoustic energy density. The monopole scattering coefficient f_1 is unaffected by viscosity, but the dipole coefficient f_2^{r} depends on viscosity through the variable $\varGamma$. As in Doinikov [11], we have $ka \ll 1$ and $ka\tilde{\delta} \ll 1$ (the wavelength is the largest length scale in the problem), but in contrast to the previous result, we have no further restriction on $\tilde{\delta}$. In the limits $\tilde{\delta} \ll 1$ and $\tilde{\delta} \gg 1$, studied by Doinikov, his results and Eq. (13) agree. For near-neutral-buoyancy particles ($\tilde{\rho} \approx 1$), the influence of viscosity on the radiation force is negligible. For the often used polystyrene microparticles ($\rho_{\mathrm{ps}} = 1.05\ \mathrm{kg/m^3}$) in pure water, the relative change in the radiation force is 0.1% for $a = 1$ µm and 0.2% for $a = 0.1$ µm. For saltwater with a salinity (near saturation) of 25% the effect increases due to increasing viscosity, and reaches 3% for $a = 1$ µm and 5% for $a = 0.1$ µm. For denser particles, e.g. pyrex glass with $\rho_{\mathrm{py}} = 2.23 \times 10^3\ \mathrm{kg/m^3}$, the influence of viscosity on the radiation force becomes important. We now find that in pure water the relative change in the radiation force is 15% for $a = 1$ µm and 33% for $a = 0.1$ µm. For saltwater with a salinity (near saturation) of 25% the effect slightly decreases due to the lowering of $\tilde{\rho}$, and reaches 11% for $a = 1$ µm and 22% for $a = 0.1$ µm. For more details on this calculation see Ref. [6].

2.2.2. Fluids with thermal expansion

The analysis is more complicated when taking the volume thermal expansion into account ($\alpha > 0, \gamma > 1$). Space limitation prevents the full expressions to be given, so we restrict ourselves to the limit $\delta_{\mathrm{th}}, \delta \ll a \ll \lambda$, corresponding to the analysis provided by Doinikov. The expression for $F^{\mathrm{rad}}_{\mathrm{1D}}$ in this limit is

$$F^{\mathrm{rad}}_{\mathrm{1D,th}} = 4\pi\left[\frac{5\tilde{\rho} - 2 - \tilde{\kappa}}{3(2\tilde{\rho}+1)} + \frac{3(\tilde{\rho}-1)^2}{(2\tilde{\rho}+1)^2}\,\tilde{\delta} - \frac{\gamma - 1}{2(1+\tilde{\Delta})}\,\tilde{\delta}_{\mathrm{th}}\right] a^3 k E_{\mathrm{ac}} \sin(2kz), \tag{14}$$

where $\tilde{\Delta} = \tilde{k}_{\mathrm{th}} / \sqrt{\tilde{D}_{\mathrm{th}}} \approx 1$ involves the particle/fluid ratios of the thermal conductivity $\tilde{k}_{\mathrm{th}}$ and diffusivity $\tilde{D}_{\mathrm{th}}$. Above, we have seen how minute the changes are in the radiation force when only viscosity is taken into account. Thus, we measure the influence of the thermal effects by the ratio R of the thermal δ_{th}-term and the viscous δ-term in Eq. (14)

$$R = \frac{(\gamma - 1)(2\tilde{\rho}+1)^2}{6(1+\tilde{\Delta})(\tilde{\rho}-1)^2}\sqrt{\frac{D_{\mathrm{th}}}{\nu}} \approx 3.1 \times 10^{-4}\ \frac{(2\tilde{\rho}+1)^2}{(\tilde{\rho}-1)^2}, \tag{15}$$

where the pre-factor is calculated for water. For neutral buoyancy ($\tilde{\rho} = 1$) the viscous term is zero and R is not defined. However, because $\gamma - 1 = 0.01$ and $\delta_{\mathrm{th}} = 0.4\delta$, the thermal effect is small ($\lesssim 1$ %). For the case of polystyrene, $\tilde{\rho} = 1.05$, we find that $R = 1.2$, and the viscous and thermal effect are of the same magnitude. However, as these two terms in Eq. (14) have opposite signs, they actually nearly cancel each other. For pyrex glass, $\tilde{\rho} = 2.23$, we obtain $R = 0.006$, and again the thermal effect is negligible. The same conclusion can be reached in the limit $\tilde{\rho} \to \infty$, because $R \to 1.2 \times 10^{-3}$.

3. Conclusions

We have analyzed the influence of thermoviscous effects on microchannel acoustofluidics. First, by including harmonic temperature-induced variations of the viscosity, we have obtained numerical results for the acoustic streaming slip velocity, which agree well with recently published analytical results by Rednikov and Sadhal [5]. The results show that thermoviscous effects increase the strength of the acoustic streaming by up to 50% for water at 80°C enclosed between parallel plane and rigid walls. Importantly, our numerical analysis can easily be extended to geometries more complex than the idealized parallel-plate geometry. Second, extending previous work by Doinikov [11], we have calculated the acoustic radiation force on a compressible, spherical micro-particle suspended in a viscous, thermal conducting fluid exposed to an ultrasound field. We have used the resulting expression to quantitatively analyze microchannel acoustophoresis, and found that for nearly-neutral-buoyancy particles, the effect of the viscosity on the radiation force disappears, while a small ($\lesssim 1\%$) thermal correction remains. For denser particles ($\tilde{\rho} > 1.05$) the effect of viscosity can be significant (larger than 30%), but the thermal effect remains a small fraction of this ($R < 0.001$).

Our results demonstrate that thermoviscous effects must be taken into account in to fully characterize ultrasound acoustofluidics.

References

[1] Friend J, Y Yeo L. Microscale acoustofluidics: Microfluidics driven via acoustics and ultrasonics. *Rev Mod Phys* 2011; **83**: 647–704.

[2] Bruus H, Dual J, Hawkes J, Hill M, Laurell T, Nilsson J, et al. Forthcoming lab on a chip tutorial series on acoustofluidics: Acoustofluidics-exploiting ultrasonic standing wave forces and acoustic streaming in microfluidic systems for cell and particle manipulation. *Lab Chip* 2011; **11**: 3579–3580.

[3] Augustsson P, Barnkob R, Wereley ST, Bruus H, Laurell T. Automated and temperature-controlled micro-piv measurements enabling long-term-stable microchannel acoustophoresis characterization. *Lab Chip* 2011; **11**: 4152–4164.

[4] Hammarstrom B, Laurell T, Nillsson J. Seed particle enabled acoustic trapping of bacteria and nanoparticles in continuous flow systems. *Lab Chip* 2012; **12**: 429-304.

[5] Rednikov AY, Sadhal SS. Acoustic/steady streaming from a motionless boundary and related phenomena: generalized treatment of the inner streaming and examples. *Journal of Fluid Mechanics* 2011; **667**: 426–462.

[6] Settnes M, Bruus H. Theoretical analysis of viscous corrections to the acoustic radiation force on cells in microchannel acoustophoresis. In: Landers J, Herr A, Juncker D, Pamme N, Bienvenue J, editors, Proc. 15th MicroTAS; pp:160–162.

[7] Muller PB, Barnkob R, Jensen MJH, Bruus H. A numerical study of microparticle acoustophoresis driven by acoustic radiation forces and streaming-induced drag forces. *Lab Chip* 2012; **12**: 4617–4627.

[8] Nyborg WL. Acoustic streaming due to attenuated plane waves. *J Acoust Soc Am* 1953; **25**: 68–75.

[9] Rayleigh L. On the circulation of air observed in Kundt's tubes, and on some allied acoustical problems, *Philosophical Transactions of the Royal Society of London* 1884; **175**: 1–21.

[10] Landau LD, Lifshitz EM. *Fluid mechanics*, 2nd ed. Oxford: Pergamon Press; 1993.

[11] Doinikov AA. Acoustic radiation force on a spherical particle in a viscous heat-conducting fluid .2. force on a rigid sphere. *J Acoust Soc Am* 1997; **101**: 722–730.